HHS Public Access

Author manuscript

Nat Cell Biol. Author manuscript; available in PMC 2009 October 12.

Published in final edited form as:

Nat Cell Biol. 2009 February ; 11(2): 211–218. doi:10.1038/ncb1829.

Phosphorylation of ATM by Cdk5 mediates DNA damage signaling and regulates neuronal death

Bo Tian[1,2], **Qian Yang**[1,2], and **Zixu Mao**[1,2,3]

[1]Departments of Pharmacology and Neurology, Emory University School of Medicine, 615 Michael Street, Atlanta, GA 30322, USA

[2]Center for Neurodegenerative Disease, Emory University School of Medicine, 615 Michael Street, Atlanta, GA 30322, USA

Abstract

The phosphatidylinositol-3-kinase-like kinase ATM (Ataxia – telangiectasia mutated) plays a central role in coordinating the DNA damage responses including cell cycle checkpoint control, DNA repair, and apoptosis. Mutations of ATM cause a spectrum of defects ranging from neurodegeneration to cancer predisposition. However, the mechanism by which DNA damage activates ATM is poorly understood. We show that Cdk5 (cyclin-dependent kinase 5), activated by DNA damage, directly phosphorylates ATM at serine 794 in postmitotic neurons. Phosphorylation at serine 794 precedes and is required for ATM autophosphorylation at serine 1981, and activates ATM kinase activity. Cdk5-ATM signal regulates phosphorylation and function of ATM targets p53 and H2AX. Interruption of Cdk5-ATM pathway attenuates DNA damage-induced neuronal cell cycle reentry and expression of p53 targets *PUMA* and *Bax*, protecting neurons from DNA damage-induced death. Thus, activation of Cdk5 by DNA damage serves as a critical signal to initiate ATM response and regulate ATM-dependent cellular processes.

DNA damage signals are transduced to activate a key family of phosphoinositide-3-kinase related kinases (PIKKs) including ATM, which phosphorylates a number of critical proteins to control cell cycle checkpoints, DNA repair, and in the case of excessive DNA damage, cell death1, 2, 3. How ATM activity is regulated by DNA damage signal is not clear. Previous studies indicate that activation of ATM involves autophosphorylation of several serine residues including S19814, 5. The widely accepted model is that autophosphorylation of ATM at S1981 releases it from the inhibitory homodimer structure, leading to its activation and recruitment to the sites of DNA double-strand break (DSB)6, but a recent report questions the role of S1987, the mouse equivalent to S1981, in DNA damage-induced activation of ATM *in vivo*7,.

[3]Correspondence should be addressed to Z.M. (zmao@pharm.emory.edu).

AUTHOR CONTRIBUTION Z. M. coordinated the overall project and planned the original experimental design. B. T. and Q. Y. conducted the experiments. Z. M. and B. T. analyzed the data and wrote the paper.

COMPETING FINANCIAL INTERESTS The authors declare that they have no competing financial interests.

Unlike proliferating cells where DNA damage typically triggers cell cycle checkpoints, postmitotic neurons under stress conditions including genotoxic stimulation activate their cell cycle machinery8. This cell cycle re-entry by postmitotic neurons leads to neuronal death and inhibition of such an ectopic cell cycle activity protects neurons9-12. Studies using ATM-/- mice show that ATM is required for the p53-mediated apoptosis of developing postmitotic neurons exposed to ionizing radiation13, 14. Suppression of ATM attenuates DNA damage agent camptothecin-induced cell cycle re-entry and death by postmitotic neurons15. These findings establish the role of ATM in DNA damage-induced neuronal death.

Cdk5, a small serine/threonine kinase regulated by activator p35 but not cell cycle, has been shown to play a role in neuronal stress response16, 17, 18. Examination of the protein sequence of ATM revealed the presence of several putative Cdk5 phosphorylation sites. We performed *in vitro* Cdk5 kinase assay by incubating purified ATM with purified Cdk5 in complex with its activator p25. Co-incubation of ATM with Cdk5 led to phosphorylation of ATM (Fig. 1a). We tested a set of GST-ATM fusion proteins and showed that GST-ATM4 (amino acid residues 772-1102) was robustly phosphorylated by Cdk5 *in vitro* (Fig. 1b). Mutation of serine 794 to alanine (S794A) abolished phosphorylation by Cdk5, suggesting that Cdk5 directly recognizes ATM S794 *in vitro*.

To demonstrate that ATM is a Cdk5 substrate in cells, we raised a phospho specific ATM antibody with a synthetic phospho-peptide corresponding to human ATM residues around S794. This phospho ATM antibody specifically detected wild type ATM when phosphorylated at S794 by Cdk5 *in vitro* but not S794A mutant (Fig. 1c). We then showed that the phospho ATM antibody detected very low background signal when ATM was expressed alone in HEK293 cells. Co-expression of Cdk5/p25 led to a strong S794 phospho signal (Fig. 1d). Interestingly, mutation of serine 1981 to alanine did not affect phosphorylation at S794, indicating that Cdk5 directly phosphorylates ATM at S794 independent of S1981.

To address how phosphorylation of ATM by Cdk5 may regulate ATM activity, we over-expressed wild type ATM with or without co-expression of Cdk5/activator in HEK293 cells, immunoprecipitated ATM, and determined ATM activity by *in vitro* kinase assay using a standard commercial substrate PHAS-I. Co-expression of Cdk5 strongly activated wt ATM while S794A mutant lost the response to Cdk5 (Fig. 2a, Supplementary information, Fig. S1a). Compared with wt ATM, the phospho mimetic mutant S794D had higher kinase activity (Fig. 2a, Supplementary information, Fig. S1b). Moreover, over-expression of Cdk5/p35 or Cdk5/p25 in HEK293 cells led to a robust activation of endogenous ATM (Fig. 2b). Thus, phosphorylation at S794 activates ATM kinase activity.

We then tested whether Cdk5 plays a role in the activation of ATM following DNA damage in primary cerebellar granule neurons (CGNs) because of their selective degeneration resulting from ATM deficiency. CGNs cultured for 7 days from postnatal day 6-7 rats were exposed to DNA damage agents known to cause DSBs in postmitotic neurons19-21. Compared to untreated control, all three DNA damage agents caused a robust activation of both Cdk5 and ATM kinase activities (Fig. 2c). In contrast, classic apoptosis inducing agent

stausporine, which typically does not cause DSBs, did not activate either Cdk5 or ATM. Tests of more general cell death inducers showed that several of them activate both Cdk5 and ATM (Supplementary information, Fig. S1). Interestingly, serum/potassium (S/K) withdrawal, another widely used model of CGN apoptosis not triggered directly by DNA damage, activated Cdk5 without affecting ATM activity. Subcellular fractionation showed that S/K withdrawal caused a delayed activation of Cdk5 only in the cytoplasm and failed to activate Cdk5 in the nucleus (Supplementary information, Fig. S1d). Together, these findings indicate that activation of Cdk5 and ATM in postmitotic neurons may represent a mode of response to a wider spectrum of signals. Since camptothecin (CPT) is very effective in activating Cdk5 and ATM under our experimental conditions, we used it as the model agent for the subsequent studies.

Because protease calpain is activated by DNA damage22 and involved in the conversion of p35 to the more potent Cdk5 activator p2523, we tested whether CPT activates Cdk5 via increasing p25. CPT treatment caused a rapid and transient increase in p25 level, which correlated with an increase in calpain activity as indicated by the cleavage of α-Fodrin (Fig. 2d). CPT-induced activation of Cdk5 paralleled the increase of p25 and preceded the activation of nuclear ATM (Fig. 2e). Inhibition of calpain with AK295 clearly reduced CPT-induced increase of p25 and activation of both Cdk5 and ATM. Collectively, these findings suggest that calpain-mediated activation of Cdk5 is required for activation of ATM in response to CPT in neurons.

Given our data in Fig. 1d, we tested whether S794 phosphorylation regulates the autophosphorylation at S1981. We found that Cdk5 increased phosphorylation at S1981 of wt ATM but failed to enhance S1981 phosphorylation of S749A mutant (Supplementary information, Fig. S1e). S794D mutant showed higher basal S1981 phosphorylation (Supplementary information, Fig. S1f). We next studied whether Cdk5 affects S1981 phosphorylation of endogenous ATM. Since our phospho ATM S794 antibody was raised using a human ATM immunogen, to achieve maximal antibody effects, we carried out the experiments in neurons differentiated from human SH-SY5Y neuroblastoma cells, known to express both Cdk5/p35 and ATM24. Compared to the low basal signal, CPT induced a rapid and robust ATM phosphorylation at S794 in differentiated SH-SY5Y neuronal cells (Fig. 3a). Closely correlated with this, CPT also caused an increase in ATM phosphorylation at S1981 with a somewhat delayed kinetics. Inhibition of Cdk5 using inhibitor roscovitine or Cdk5 RNAi adenovirus blocked CPT-induced phosphorylation at S794 and S1981 (Fig. 3a-b), indicating that Cdk5-mediated S794 phosphorylation precedes and is required for ATM autophosphorylation at S1981.

Next, we tested the effects of inhibiting Cdk5 on ATM-mediated phosphorylation of its two well-characterized substrates, p53 and H2AX. Exposure of CGNs to CPT increased p53 phosphorylation at S15, a known site targeted directly by ATM but not by Cdk5 (Supplementary information, Fig. S1g-h). Inhibition of Cdk5 by roscovitine or RNAi significantly attenuated CPT-induced ATM activity and p53 phosphorylation at S15 (Fig. 3c-d). Immunocytochemistry studies showed that CPT induces robust formation of γ-H2AX foci in CGNs. Both roscovitine and Cdk5 RNAi efficiently reduced the number of CPT-

induced γ-H2AX foci (Fig. 3e-f). These data suggest that ATM-mediated phosphorylation of p53 and formation of γ-H2AX foci following DSBs requires Cdk5.

As proline-directed serine/threonine kinase, Cdk5 and other cycle cell related Cdks share the same basic phosphorylation recognition motif. This raised the possibility that other Cdks may also regulate ATM directly. To test this, we re-confirmed the specificity of immunoprecipitation (Supplementary information, Fig. S1i) and showed that maximal activation of Cdk5 occurs 30 min after CPT exposure and precedes ATM activity, which peaks at 60 min (Fig. 4a), and γH2AX foci formation (Supplementary information, Fig. S2). In comparison, while CPT did activate Cdk2 and 6, their activation did not peak until 2 hr after treatment. Furthermore, *in vitro* kinase assays showed that neither purified Cdk2 nor Cdk6 phosphorylates ATM S794 under the experimental conditions when they robustly phosphorylated control substrate Histone H1 (Fig. 4b). Dominant negative Cdk2 and 6 had little effects on CPT-induced γ-H2AX foci formation in CGNs while dnCdk5 effectively reduced the number of γ-H2AX foci (Fig. 4c). The sequential activation of Cdk5, ATM and Cdk2/6 after DSBs suggests that Cdk2 and 6 do not participate in the initial activation of ATM in CGN model.

Previous studies showed that postmitotic neurons re-express cell cycle markers including Cdk2 and 6 in response to a variety of neuronal death signals including DNA damage8, 10. Our findings in Figure 3a suggested that Cdk5-mediated activation of ATM may be required for stress-induced cell cycle re-entry of postmitotic neurons. Analysis by Real-Time RT-PCR showed that CPT increased Cdk2 and 6 mRNA levels in CGNs while roscovitine clearly blocked such increases as early as 30 min after CPT, which coincides with the peak activity of Cdk5 and precedes significantly the activation of Cdk2 and 6 (Fig. 4a, d, e). This suggests that Cdk5 is responsible for DNA damage-induced re-expression of Cdk2 and 6. Cell cycle analysis by flow cytometry showed that CPT caused a significant number of postmitotic CGNs and differentiated SH-SY5Y neurons to re-enter S phase, which was reduced by roscovitine, Cdk5 RNAi, or ATMi [Fig. 4f, 4g. Supplementary information, Fig. S3A. ATM inhibitors WM and CA had the same effects (data not shown)]. We measured cell cycle using a second method, BrdU labeling, to confirm these findings (Supplementary information, Fig. S3B). Collectively, these results indicate that Cdk5-ATM regulates DNA damage-induced reactivation of cell cycle machinery in postmitotic neurons.

Transcription factor p53 is a key ATM substrate that mediates DNA damage response. Our findings that inhibition of Cdk5 reduces ATM-mediated phosphorylation of p53 suggest that Cdk5 may regulate p53 function via ATM in response to DNA damage. We assessed p53 activity by a luciferase reporter assay in a background without endogenous functional ATM (A-T cells) and in CGNs. Our data showed that DNA damage-induced activation of p53 in CGNs is dependent on Cdk5. ATM mediates Cdk5-induced full activation of p53 activity, which requires S794 but not S1981. These data and related text are included in Supplementary information, Fig. S4.

In response to DNA damage and ATM signaling, p53 activates the expression of many critical downstream target genes related to death including *puma* and *bax*25. Real-Time RT-PCR analysis showed that CPT leads to a significant increase in the mRNA levels of both

puma and *bax* while roscovitine reduced *puma* and *bax* mRNA to near basal levels. Similar results were obtained for additional p53 targets such as PCNA25 (Supplementary information, Fig. S5a-c). Together, these findings indicate that Cdk5 is required for mediating CPT-induced ATM dependent expression of p53 target gene expression.

Our above findings suggest that phosphorylation of ATM by Cdk5 plays a key role in DNA damage-induced neuronal death. We tested this by performing WST-1 survival assays. Our data showed that CPT significantly reduces the survival of CGNs while roscovitine is sufficient to block CPT-induced death of CGNs dose-dependently (Fig. 5a). Roscovitine and KU-5593326 also reduced CPT-induced CGN death in a time-dependent manner (Fig. 5b). In agreement with these, inhibition of calpain also protected CGNs from CPT toxicity (Fig. 5c).

To corroborate these findings, we showed that both knocking down Cdk5 or ATM by RNAi and over-expressing the dnCdk5 or kdATM significantly attenuates CPT-induced neuronal death (Fig. 5d-e, Supplementary information, Fig. S5d). Furthermore, ATM mutant S794A effectively decreased CPT-induced neuronal death in differentiated SH-SY5Y cells as well (Fig. 6f). These findings indicate that phosphorylation of ATM at S794 by Cdk5 directly modulates CPT-induced death process in neurons.

Proper signaling the presence of DSBs requires conversion of the dormant ATM to its highly active form. Our study establishes phosphorylation of ATM at S794 by Cdk5 as a critical step in mediating DNA damage-induced ATM activation in postmitotic neurons. S794 phosphorylation precedes and is required for ATM autophosphorylation at S1981, indicating that S794 phosphorylation is a more upstream initiation event. How phosphorylation at S794 leads to ATM activation is not presently clear. It is conceivable that part of the subsequent changes following S794 phosphorylation may also involve regulation of intermolecular interactions of ATM molecules. Whether S794 phosphorylation regulates the recruitment of ATM to the site of DNA strand break by MRN complex 27-31 and participates DNA repair requires further investigation.

Our studies used postmitotic neurons as a model. Whether phosphorylation of ATM by Cdk5 is limited to neural tissue remains to be addressed. Since both Cdk5 and ATM are widely expressed by a variety of cell types including cancers, it raises the possibility that Cdk5-ATM pathway may be engaged following DNA damage in broad tissue types. Our findings that agents not known to induce DNA damage such as chloroquine or mild osmotic shock can also activate Cdk5-ATM pathway (Supplementary information, Fig. S6) suggests that Cdk5-mediated regulation of ATM may play a role in cellular response to a broad spectrum of signals.

Cdk5 and ATM are detected in both cytoplasmic and nuclear compartments in neurons. It is interesting to note that although CPT activates Cdk5 in both cytoplasm and nucleus, only nuclear ATM exhibits significant activation under the same condition. Similarly, KCl withdrawal induced robust activation of Cdk5 in the cytoplasm. But this failed to cause significant change of ATM in either the cytoplasm or nucleus. Thus, it appears that under

the experimental conditions tested, Cdk5 preferentially activates ATM in the nucleus. This may constitute at least part of a process allowing cells to critically distinguish stress signals.

METHODS

Cell culture

Cerebellar granule neurons (CGNs) were cultured from Long Evans rats at postnatal day 6 or 7 on plates coated with poly-L-lysine (Sigma- Aldrich) 17. CGNs were maintained in Basal Medium Eagle containing 10% dialyzed FBS, 25 mM KCl, 0.1 mg/ml gentamycin, 2 mM glutamine, and 25 mM glucose. Treatments or transfection performed 7 days after plating. HEK293 cells and AT cells (GM05849C cell line, a human ATM-deficient fibroblasts) were cultured in DMEM supplemented with 10% FBS. Human SH-SY5Y cells were cultured in DMEM/F-12 supplemented with 10% FBS, and differentiated with 10 μM all-trans-retinoic acid (Sigma-Aldrich) for 6 days and then 2nM brain-derived neurotrophic factor (BDNF, Sigma-Aldrich) for another 2 days as described previously 32.

Chemicals and antibodies

Roscovitine, wortmannin, caffeine, calcium ionopore, glutamate were purchased from Sigma-Aldrich. H_2O_2 and Hoechst 33258 were from Fisher Scientific. KU-55933 was provided by KuDos. AK-295 was kindly provided by Dr. Jonathan D. Glass. For immunoblotting, rabbit polyclonal anti-p53, mouse monoclonal anti-phospho-p53 (Ser15), rabbit polyclonal anti-actin, rabbit polyclonal anti-Cdk2, and mouse monoclonal anti-Cdk6 are all from Cell signaling; mouse monoclonal anti-ATM is from Sigma-Aldrich; rabbit polyclonal anti-ATM from Calbiochem; rabbit polyclonal anti-p35 (N-20) from Santa Cruz; and mouse monoclonal anti-Cdk5 from Neomakers. For Immunofluorescent staining, mouse monoclonal anti-γH2AX are from Upstate Biotechnology; rabbit polyclonal anti-GFP from Abcam and fluorescent secondary antibodies from Jackson ImmunoResearch.

Generation of antibody to phosphor-Ser794 ATM

Rabbit polyclonal phosphospecific antibody against ATM Ser794 was produced by 21st Century Biochemicals with a synthetic 16mer phosphopeptide (KLH-coupled) corresponding to residues surrounding Ser794 of human ATM (Acetyl-CLSNATKpSPNKIASG-amide).

Constructs and recombinant proteins

Constructs encoding GST-fusion ATM fragments were kindly provided by Dr. Martin L. Lavin33. A plasmid encoding an N-terminal Flag-tagged ATM protein was a kind gift of Dr. Michael Kastan34. Serine 794 and 1981 mutation to alanine (SA) or glutamine (SD) was performed using QuikChange site-directed II mutagenesis kit (Stratagene). Recombinant GST-fusion proteins were induced and purified from BL21 (DE3) competent cells (Invitrogen).

Plasmid transfection

Primary CGNs were transceintly transfected using Calcium Phosphate ProFection Mammalian Transfection system (Promega) according to the manufacturer's instructions. HEK293 and A-T cells were transfected using Lipofectamine 2000 reagents (Invitrogen). Drug treatments were performed 24 hours after transfection.

Adenoviruses and infection

Human CDK5, ATM and control RNAi Adenovirus were purchased from Millipore. Viruses were added to SH-SY5Y cells after RA-BDNF differentiation. Treatments were performed 24 hours after infection.

Cdk5 shRNA lentivirus and infection

To construct the 19 nucleotide (corresponding to rat Cdk5 nt positions 639-657) 35 hairpin siRNA cassettes, two complementary DNA oligonucleotides were chemically synthesized in Invitrogen, annealed, and inserted into pSUPER shuttle vector immediately downstream of the H1 RNA pol III promoter: 5'-GATCCCC- GAGGATCTTTCGACTGCTA-TTCAAGAGA-TAGCAGTCGAAAGATCCTC-TTTTTGGAAA-3 ' a n d 5 '-AGCTTTTCCAAAAA-GAGGATCTTTCGACTGCTA-TCTCTTGAA-TAGCAGTCGAAAGATCCTC-GGG-3'. The RNAi cassettes with H1 promoter were amplified by PCR and subcloned into pFUGW transfer vector 36. Lentiviruses were produced in HEK293T cells by cotransfection of pFUGW-CDK5i, packaging plasmid p8.91, vesicular stomatitis virus (VSV) envelope expression plasmid (pMD.G). Lentiviruese were concentrated and tittered on HEK293T cells. Serial dilutions of the virus were test to get the highest infectivity. Lentiviruses were applied to CGNs at the 4th day *in vitro* (DIV) and treatments were performed 72 hours after infection.

Subcellular fractionation

Cytoplasmic and nuclear fractionation was performed using EZ Nuclei Islation Kit (Sigma-Aldrich) according to manufacturer's protocol, which involves three cycles of thorough cell lysis and washing. Only the first cytoplasmic lysate and the last nuclear lysate were kept and used in experiments.

Immunoprecipitation and Immunoblotting

Lysates were generally prepared with NP-40 lysis buffer (20 mM Tris, pH 8.0, 135 mM NaCl, 1 mM $MgCl_2$, 0.1 mM $CaCl_2$, 10% glycerol, 1% NP-40, 0.1 mM Na_3VO_4, 50 mM ß-glycerol phosphate, 10 mM NaF, and protease inhibitors from Roche). Fifty to one hundred micrograms of protein were used for immunoblotting by SDS-PAGE analysis and one hundred to five hundred micrograms of protein were used for immunoprecipitation to incubate with 1 to 2 μg corresponding antibody at 4°C overnight. The immune complexes were collected with protein G Plus/Protein A-Agarose (Calbiochem) and washed three times with NP-40 lysis buffer.

ATM and Cdk Kinase Assays

Active Cdk5/p25, Cdk2/cyclin A, or Cdk6/cyclin D3 kinases were purchased from Upstate Biotechnology. In vitro Cdk kinase assay were performed following the manufacturer's instructions. Briefly, two microgram purified ATM or GST-ATM4 fragment recombinant proteins were incubated with active Cdk kinase in Cdk kinase buffer (8 mM MOPS/NaOH pH7.0, 200 nM EDTA) containing 20 μM ATP, 10 μCi of [γ-^{32}P]-ATP for 15 min at 30°C. To determine kinase activity of ATM or Cdks in cells, corresponding immunoprecipitates were washed twice with either ATM kinase buffer (50 mM HEPES, pH 7.5, 150 mM NaCl, 4 mM $MnCl_2$, 10% glycerol, 1 mM dithiothreitol, and 100 μM Na_3VO_4) or Cdk kinase buffer, and incubated in the kinase buffer containing [γ-^{32}P]-ATP and 1 μg of substrate [PHAS-I for ATM kinase assay (Calbiochem) and histone H1 for Cdk kinase assay (Upstate)] for 30 min at 30°C. The reaction was stopped with SDS sample buffer and 5 min boiling. Phosphorylation of substrates after SDS-PAGE was analyzed by autoradiography.

Cell Cycle Analysis

Cells were harvested by trypsinization, fixed, and stained with propidium iodide. Total DNA content was analyzed on a FACSCalibur flow cytometer (Becton Dickinson) using the programs BD CompBeads plus BD FACSDiva and FlowJo.

Survival Assays

WST-1 assay (Roche) was performed following the manufacturer's instructions. Briefly, cells were cultured in 24 well plates. After treatments, incubate cells with WST-1 substrate, a ready-to-use substrate which measures the metabolic activity of viable cells, for 1–4 hours, followed by spectrophotometric assay of colored product. Single-cell survival assays were performed using Viability/Cytotoxicity Kit (Invitrogen). Briefly, CGNs were stained with ethidium homodimer-1 (EthD-1) without permeabilization. GFP-positive cells with or without EthD-1 staining were counted using Olympus IX51 fluorescence microscope in a blind manner. Two hundred or more transfected cells were counted for each treatment. Rates of dead CGNs were calculated as percentage of cells with co-localization of EthD1 and GFP in the total number of GFP-positive cells counted.

Luciferase Assays

Transient transfections were performed by the calcium phosphate transfection method (Sigma-Aldrich) as described by the manufacturer with PG13pyLuc (wild-type p53 reporter) and its corresponding mutant MG13pyLuc (mutant p53 reporter) 37. The amount of DNA transfected was equalized by addition of a control vector. Treatments were performed 24 h posttransfection. Cell lysates were analyzed using Enhanced Luciferase Assay Kit (BD Bioscience) according to the manufacturer's instruction.

Immunofluorescence

CGNs were cultured on cover glasses coated with poly-L-lysine. Cells were fixed with 3.7% neutral buffered formalin and permeabilized with 0.3% Triton X-100 in PBS, blocked in 5% normal goat serum, and were stained with anti-γH2AX or anti-GFP followed by corresponding fluorescent secondary antibodies (Jackson ImmunoResearch). Cells were

counterstained with Hoechst 33258, mounted with Vectashield mounting medium (Vector Laboratories), and then analyzed with an Olympus BX51 fluorescence microscope. Numbers of γ-H2AX foci in two hundred or more CGNs were counted.

Quantitative Real-Time reverse transcription-polymerase chain reaction (qRT-PCR)

For real-time RT-PCR, the total RNA was extracted using TRIzol reagent (Invitrogen). Total RNA (1 μg) of each sample was reversely transcribed using SuperScript™ First-Strand Synthesis SuperMix for qRT-PCR (Invitrogen) in a 20 ml volume. The amplification was carried out in a total volume of 50 μL containing 1ml of each primer, 25 ml Platinum SYBR Green qPCR SuperMix-UDG (invitrogen) 1ml ROX reference dye, and 2 μL of 1:10 diluted cDNA using ABI PRISM 7000 Real-Time PCR Systems according to the manufacturer's instructions. In each experiment, the 18S ribosome RNA (18S rRNA) was amplified as a reference standard. Primer sets were designed using OligoPerfect program (Invitrogen). 18S rRNA primers were 18S rRNA-F, 5'-AACGGCTACCACATCCAA-3 ' ; 1 8 S r R N A-R, 5'-GACTCATTCCAATTACAGGGC-3'. Other target gene primers were BAX-F, 5'-TGTTGCTGATGGCAACTTC-3'; BAX-R, 5 '-GATCAGCTCGGGCACTTTAG-3'; PUMA-F, 5 '- GCGGAGACAAGAAGAGCAAC-3 ' ; P U M A-R, 5 '-CTCCAGGATCCCTGGGTAAG-3'; Cdk2-F, 5'- CATTCCTCTTCCCCTCATCA-3'; Cdk2-R, 5 '-TACCAGAGGGTCACCACCTC-3 ' ; C d k 6-F, 5 '-TGTTTCAGCTTCTCCGAGGT-3'; Cdk6-R, 5'-GGCTTTCTGCGAAACAGTTC-3'; p21-F, 5 '- TGGACAGTGAGCAGTTGAGC-3 ' ; P 2 1-R, 5 '-ACACGCTCCCAGACGTAGTT; PCNA-F, 5'- TTGGAATCCCAGAACAGGAG-3'; PCNA-R, 5'- AGAAAACTTCACCCCGTCCT-3'. All PCR reactions were performed in duplicate. Standard curves (cycle threshold values versus template concentration) were prepared for each target gene and for the endogenous reference (18S rRNA) in each sample. To confirm the specificity of the PCR reaction, PCR products were electrophoresed on a 1.2% agarose gel.

Statistical analysis

The results were analyzed using by two-tailed Student's T test where appropriate.

Supplementary Material

Refer to Web version on PubMed Central for supplementary material.

Acknowledgments

We thank Drs. Bert Vogelstein, Richard Gatti, Michael Kastan, Martin Lavin, and Shuki Mizutani for p53 reporter constructs, purified ATM protein, ATM mammalian expression constructs, GST-ATM expression constructs, and A-T cell lines, respectively. This work was partially supported by NIH grants R01 NS048254 (Z. M.) and R01 AG023695 (Z. M.) and The Robert W. Woodruff Health Sciences Center Fund (Z. M.).

References

1. McKinnon PJ. ATM and ataxia telangiectasia. EMBO Rep. 2004; 5:772–776. [PubMed: 15289825]
2. Khanna KK, Lavin MF, Jackson SP, Mulhern TD. ATM, a central controller of cellular responses to DNA damage. Cell Death Differ. 2001; 8:1052–1065. [PubMed: 11687884]

3. Roos WP, Kaina B. DNA damage-induced cell death by apoptosis. Trends Mol Med. 2006; 12:440–450. [PubMed: 16899408]
4. Bakkenist CJ, Kastan MB. DNA damage activates ATM through intermolecular autophosphorylation and dimer dissociation. Nature. 2003; 421:499–506. [PubMed: 12556884]
5. Kozlov SV, et al. Involvement of novel autophosphorylation sites in ATM activation. Embo J. 2006; 25:3504–3514. [PubMed: 16858402]
6. Dupre A, Boyer-Chatenet L, Gautier J. Two-step activation of ATM by DNA and the Mre11-Rad50-Nbs1 complex. Nat Struct Mol Biol. 2006; 13:451–457. [PubMed: 16622404]
7. Pellegrini M, et al. Autophosphorylation at serine 1987 is dispensable for murine Atm activation in vivo. Nature. 2006; 443:222–225. [PubMed: 16906133]
8. Park DS, Levine B, Ferrari G, Greene LA. Cyclin dependent kinase inhibitors and dominant negative cyclin dependent kinase 4 and 6 promote survival of NGF-deprived sympathetic neurons. J Neurosci. 1997; 17:8975–8983. [PubMed: 9364045]
9. Liu DX, Greene LA. Neuronal apoptosis at the G1/S cell cycle checkpoint. Cell Tissue Res. 2001; 305:217–228. [PubMed: 11545259]
10. Park DS, et al. Cyclin-dependent kinases participate in death of neurons evoked by DNA-damaging agents. J Cell Biol. 1998; 143:457–467. [PubMed: 9786955]
11. Copani A, et al. Activation of cell-cycle-associated proteins in neuronal death: a mandatory or dispensable path? Trends Neurosci. 2001; 24:25–31. [PubMed: 11163884]
12. Herrup K, Neve R, Ackerman SL, Copani A. Divide and die: cell cycle events as triggers of nerve cell death. J Neurosci. 2004; 24:9232–9239. [PubMed: 15496657]
13. Herzog KH, Chong MJ, Kapsetaki M, Morgan JI, McKinnon PJ. Requirement for Atm in ionizing radiation-induced cell death in the developing central nervous system. Science. 1998; 280:1089–1091. [PubMed: 9582124]
14. Lee Y, Chong MJ, McKinnon PJ. Ataxia telangiectasia mutated-dependent apoptosis after genotoxic stress in the developing nervous system is determined by cellular differentiation status. J Neurosci. 2001; 21:6687–6693. [PubMed: 11517258]
15. Kruman II, et al. Cell cycle activation linked to neuronal cell death initiated by DNA damage. Neuron. 2004; 41:549–561. [PubMed: 14980204]
16. Dhavan R, Tsai LH. A decade of CDK5. Nat Rev Mol Cell Biol. 2001; 2:749–759. [PubMed: 11584302]
17. Tang X, et al. Cyclin-dependent kinase 5 mediates neurotoxin-induced degradation of the transcription factor myocyte enhancer factor 2. J Neurosci. 2005; 25:4823–4834. [PubMed: 15888658]
18. Gong X, et al. Cdk5-mediated inhibition of the protective effects of transcription factor MEF2 in neurotoxicity-induced apoptosis. Neuron. 2003; 38:33–46. [PubMed: 12691662]
19. Wu J, Liu LF. Processing of topoisomerase I cleavable complexes into DNA damage by transcription. Nucleic Acids Res. 1997; 25:4181–4186. [PubMed: 9336444]
20. Xiao H, et al. The topoisomerase IIbeta circular clamp arrests transcription and signals a 26S proteasome pathway. Proc Natl Acad Sci U S A. 2003; 100:3239–3244. [PubMed: 12629207]
21. Pommier Y. Topoisomerase I inhibitors: camptothecins and beyond. Nat Rev Cancer. 2006; 6:789–802. [PubMed: 16990856]
22. Sedarous M, et al. Calpains mediate p53 activation and neuronal death evoked by DNA damage. J Biol Chem. 2003; 278:26031–26038. [PubMed: 12721303]
23. Lee MS, et al. Neurotoxicity induces cleavage of p35 to p25 by calpain. Nature. 2000; 405:360–364. [PubMed: 10830966]
24. Li BS, Zhang L, Gu J, Amin ND, Pant HC. Integrin alpha(1) beta(1)-mediated activation of cyclin-dependent kinase 5 activity is involved in neurite outgrowth and human neurofilament protein H Lys-Ser-Pro tail domain phosphorylation. J Neurosci. 2000; 20:6055–6062. [PubMed: 10934255]
25. Rozan LM, El-Deiry WS. p53 downstream target genes and tumor suppression: a classical view in evolution. Cell Death Differ. 2007; 14:3–9. [PubMed: 17068503]
26. Hickson I, et al. Identification and characterization of a novel and specific inhibitor of the ataxia-telangiectasia mutated kinase ATM. Cancer Res. 2004; 64:9152–9159. [PubMed: 15604286]

27. Gupta A, et al. Involvement of human MOF in ATM function. Mol Cell Biol. 2005; 25:5292–5305. [PubMed: 15923642]
28. Sun Y, Jiang X, Chen S, Fernandes N, Price BD. A role for the Tip60 histone acetyltransferase in the acetylation and activation of ATM. Proc Natl Acad Sci U S A. 2005; 102:13182–13187. [PubMed: 16141325]
29. Uziel T, et al. Requirement of the MRN complex for ATM activation by DNA damage. Embo J. 2003; 22:5612–5621. [PubMed: 14532133]
30. Kitagawa R, Bakkenist CJ, McKinnon PJ, Kastan MB. Phosphorylation of SMC1 is a critical downstream event in the ATM-NBS1-BRCA1 pathway. Genes Dev. 2004; 18:1423–1438. [PubMed: 15175241]
31. Falck J, Coates J, Jackson SP. Conserved modes of recruitment of ATM, ATR and DNA-PKcs to sites of DNA damage. Nature. 2005; 434:605–611. [PubMed: 15758953]
32. Jamsa A, Hasslund K, Cowburn RF, Backstrom A, Vasange M. The retinoic acid and brain-derived neurotrophic factor differentiated SH-SY5Y cell line as a model for Alzheimer's disease-like tau phosphorylation. Biochem Biophys Res Commun. 2004; 319:993–1000. [PubMed: 15184080]
33. Khanna KK, et al. ATM associates with and phosphorylates p53: mapping the region of interaction. Nat Genet. 1998; 20:398–400. [PubMed: 9843217]
34. Lim DS, et al. ATM binds to beta-adaptin in cytoplasmic vesicles. Proc Natl Acad Sci U S A. 1998; 95:10146–10151. [PubMed: 9707615]
35. Meuer K, et al. Cyclin-dependent kinase 5 is an upstream regulator of mitochondrial fission during neuronal apoptosis. Cell Death Differ. 2007; 14:651–661. [PubMed: 17218957]
36. Lois C, Hong EJ, Pease S, Brown EJ, Baltimore D. Germline transmission and tissue-specific expression of transgenes delivered by lentiviral vectors. Science. 2002; 295:868–872. [PubMed: 11786607]
37. el-Deiry WS, et al. WAF1, a potential mediator of p53 tumor suppression. Cell. 1993; 75:817–825. [PubMed: 8242752]

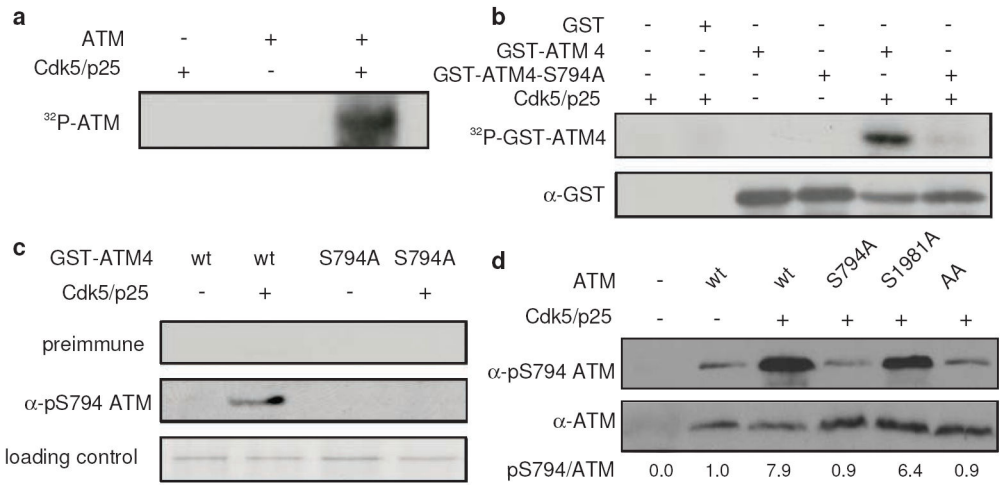

Figure 1. Cdk5 directly phosphorylates ATM *in vitro* and in cells

(**a**) Phosphorylation of purified ATM protein by Cdk5/p25 *in vitro*. (**b**) Phosphorylation of ATM by Cdk5 at S794 *in vitro*. Purified recombinant GST-ATM4 (aa772 ~aa1102) and S794 to Alanine mutant (GST-ATM4-S794A) were phosphorylated by purified Cdk5/p25 *in vitro* (top panel). The same membrane was probed with α-GST antibody as loading control (bottom panel). (**c**) Characterization of phosphospecific ATM S794 antibody. GST-ATM4 and GST-ATM4-S794A either unphosphorylated or phosphorylated with cold ATP by purified Cdk5/p25 *in vitro* were probed with preimmune serum (top panel) and ATM S794 phosphospecific antibody (middle panel). Coomassie blue staining of substrate shows loading control (bottom panel). (**d**) Phosphorylation of ATM by Cdk5 at S794 in cells. Cdk5/p25 and ATM [wild type (wt) or S794A, S1981A, S794A/S1981A (AA) mutants] were transfected into HEK293 cells as indicated. Phospho-S794 levels in the lysates were determined by immunoblotting using phospho-specific antibody (top panel). The same membrane was re-probed for total ATM (bottom panel).

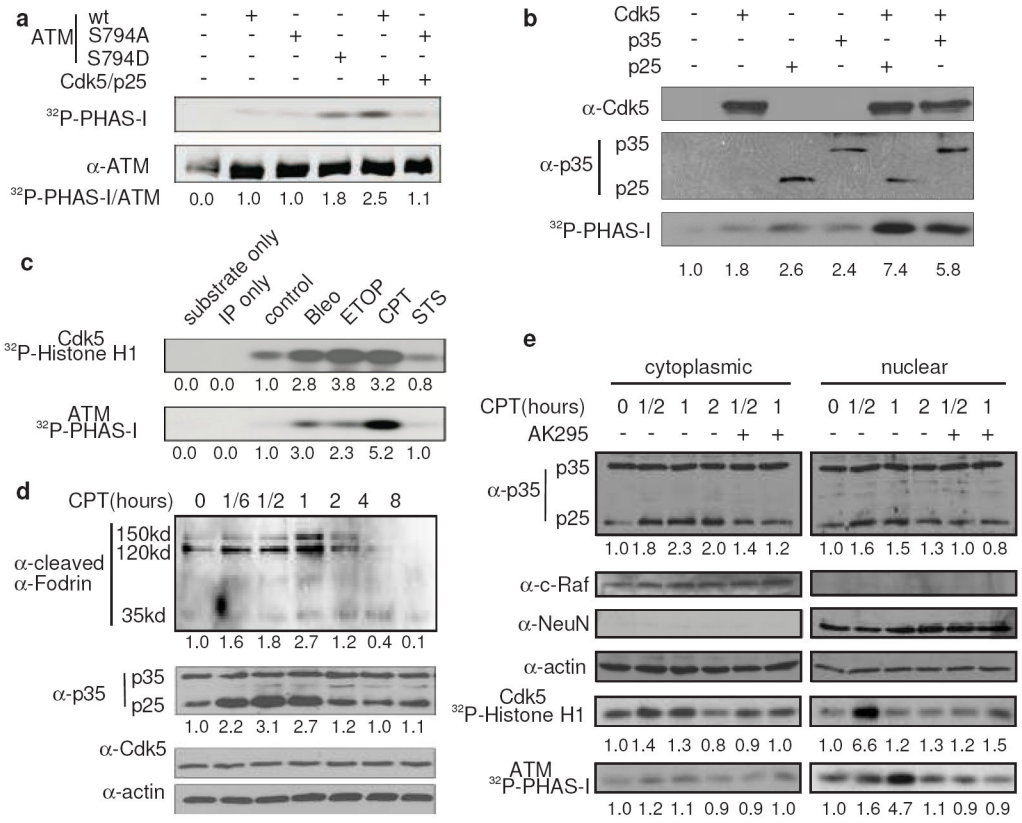

Figure 2. Activation of Cdk5 by calpain contributes to DNA damage-induced ATM activation

(**a**) Activation of ATM by Cdk5 mediated phosphorylation. HEK293 cells were transfected with Cdk5/p25 and ATM (wt, S794A and S794D mutants) as indicated. After 24 hours, ATM kinase activity was measured. The bottom panel shows the equal expression of ATM used in the lysates. The numbers are relative values with control set to one (same hereafter). (**b**) Activation of endogenous ATM by Cdk5/p25 or Cdk5/p35. Cdk5, p25 and p35 were overexpressed in HEK293 cells as indicated. After 24 hours, the levels of overexpressed proteins (top two panels) and ATM kinase activities (bottom panel) were determined. (**c**) Activation of Cdk5 and ATM by DNA damage. CGNs were treated with 10 μM camptothecin (CPT), 10 μM etoposide (Etop), 100 μg ml-1 bleomycin (Bleo), or 2 μM stausporine (STS) for 1 hour. Cdk5 and ATM kinase activity were measured using Histone H1 and PHAS-I as substrate, respectively. (**d**) CPT-induced p35 degradation. CGNs were treated with 10 μM CPT for the indicated periods of time. Level of cleaved α-fodrin, p35, p25 and Cdk5 were measured by immunoblotting. (**e**) Effects of inhibiting calpain on DNA damage-induced Cdk5 and ATM activation. CGNs were treated with or without 50 μM calpain inhibitor AK295 for 30 min and then with 10 μM CPT for the indicated periods of time. Cytoplamic and nuclear lysates were used for the determination of the levels of p35 and p25, and Cdk5 and ATM kinase activities. The membranes were reprobed for c-Raf, NeuN and actin as cytoplasmic fraction, nuclear fraction and loading controls, respectively.

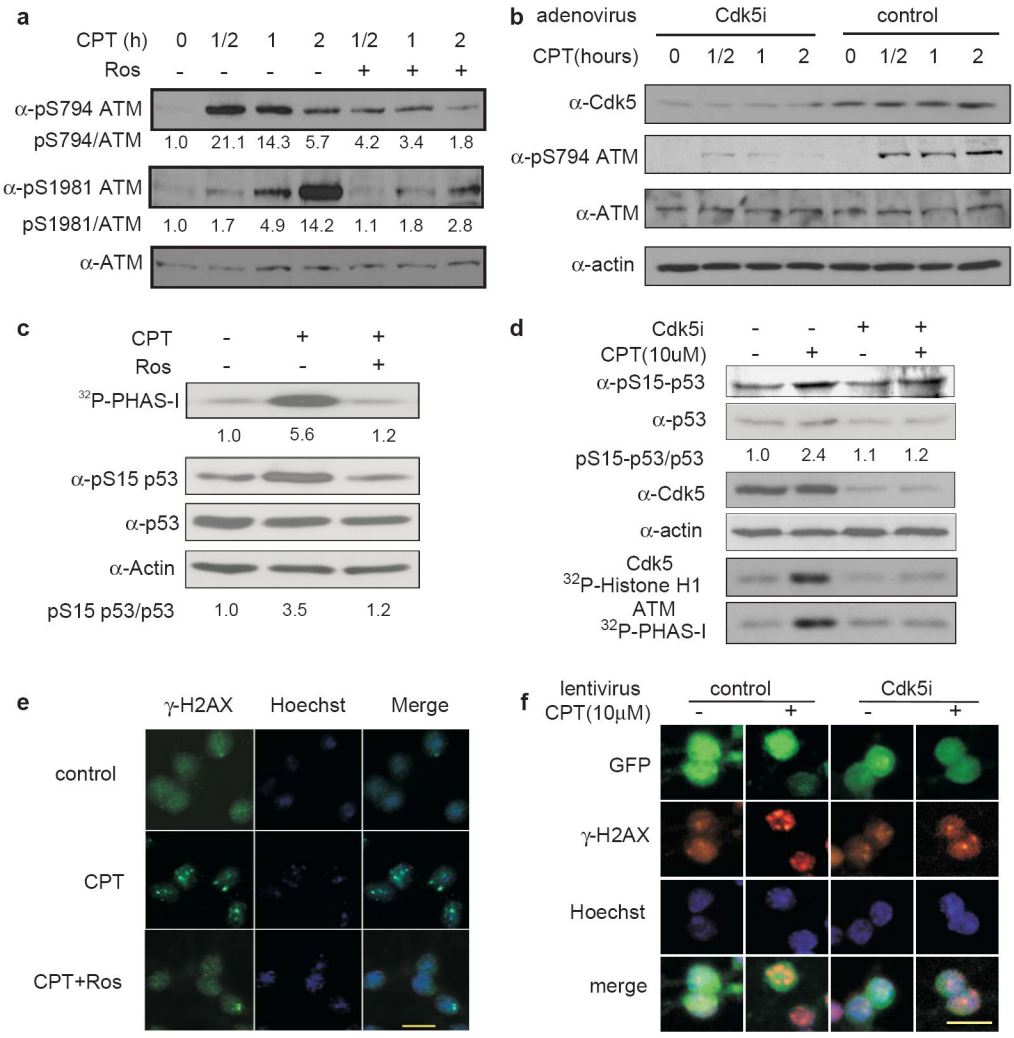

Figure 3. Inhibition of Cdk5 blocks DNA damage-induced phosphorylation and activation of ATM and its effects on downstream targets

(**a**) Inhibition of CPT-induced ATM phosphorylation at S794 and S1981 by roscovitine. Neurons differentiated from SH-SY5Y cells were pretreated with or without 10 μM roscovitine (Ros) for 30 min and followed with 10 μM CPT for the indicated periods of time. Phospho-S794, phospho-S1981 and total ATM were determined by immunoblotting. (**b**) Inhibition of CPT-induced ATM phosphorylation at S794 and S1981 by knocking down Cdk5. Neurons differentiated from SH-SY5Y cells were infected with control or Cdk5 RNAi adenovirus for 24 hours, and then treated with 10 μM CPT for the indicated periods of time. Cdk5, phospho-S794, phospho-S1981, total ATM and actin were determined by immunoblotting. (**c**) Inhibition of CPT-induced ATM activation and p53 phosphorylation by roscovitine. CGNs were treated with or without 10 μM Roscovitine for 30 min and then with 10 μM CPT treatment for 1 hour. ATM kinase activity, phospho-S15, total p53 and actin were measured in the same set of lysates. (**d**) Inhibition of CPT-induced ATM activation and p53 phosphorylation by knocking down Cdk5. CGNs were infected with Cdk5i or scrambled RNAi lentivirus for 72 hours and then treated with 10 μM CPT treatment for 1 hour. Cdk5 and ATM kinase activities and levels for Cdk5, phospho-S15, total p53 and actin were

measured in the same set of lysates. (**e**) Reduction of CPT-induced γ-H2AX foci formation by roscovitine. CGNs were treated with or without 10 μM Roscovitine (Ros) for 30 min and then exposed to 10 μM CPT for 1 hour. γ-H2AX (green) was detected by immunocytochemistry, and nuclei were labeled with Hoechst (blue). The average numbers of foci/cell counted blindly are control, 0.26; CPT, 3.91; CPT+Ros, 1.08 ($p < 0.001$). (**f**) Reduction of CPT-induced γ-H2AX foci formation by knocking down Cdk5. CGNs were infected with CDK5 RNAi or control lentivirus for 72 hours and then exposed to 10 μM CPT for 1 hour. γ-H2AX (red) and GFP (green) were detected by immunocytochemistry, and nuclei were labeled with Hoechst (blue). The scale bars represent 10 μm. The average numbers of foci/cell counted blindly are control, 0.21; control+CPT, 3.00; Cdk5i, 0.13; Cdk5i+CPT, 1.22 ($p < 0.001$).

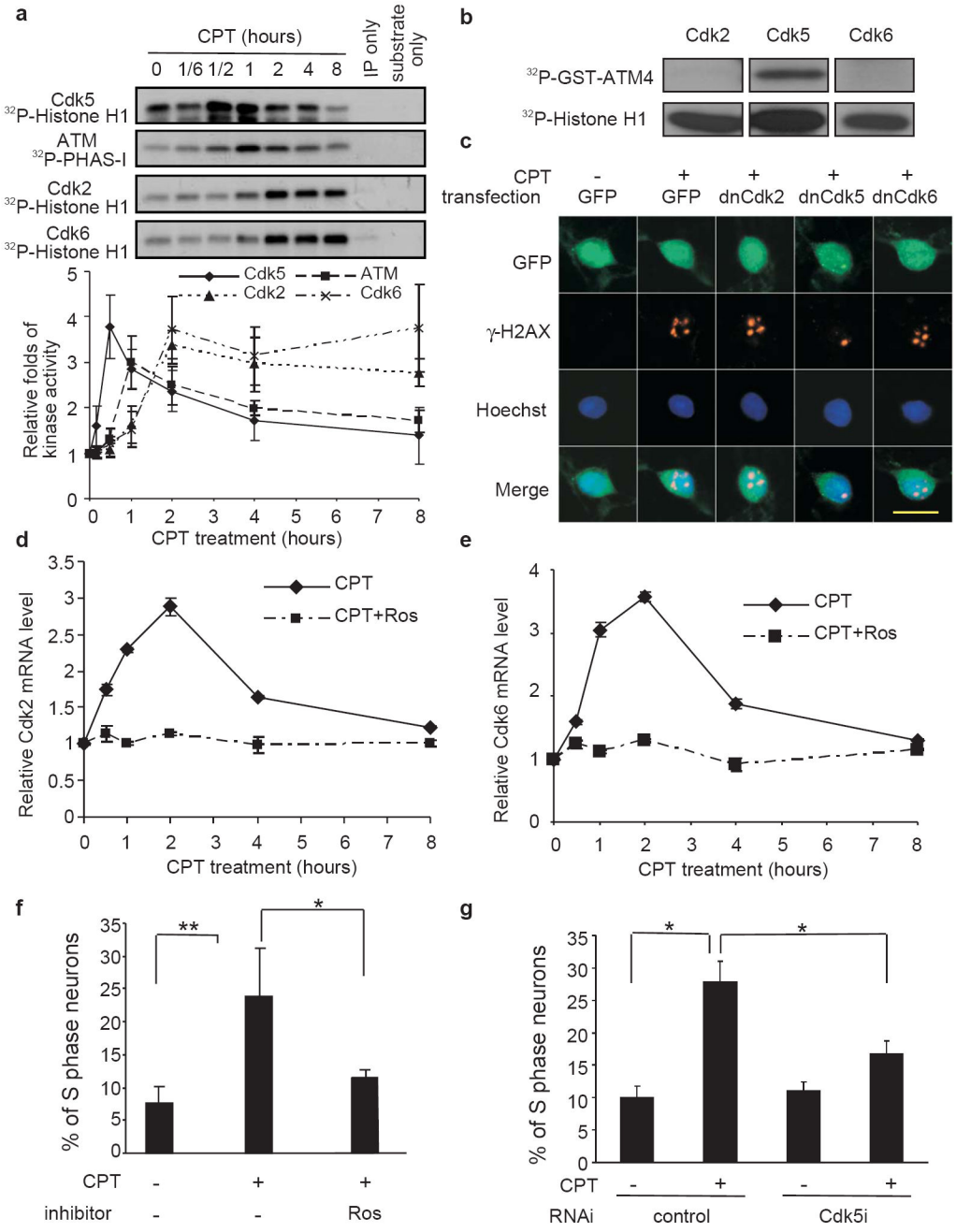

Figure 4. Cdk5 regulates CPT-induced the re-entry of cell cycle by postmitotic neurons

(**a**) Kinetics of CPT-induced activation of Cdks and ATM. CGNs were treated with 10 μM CPT for the indicated periods of time. Cdk5, ATM, Cdk2 and Cdk6 kinase activities were measured following immunoprecipitation. The lower graph is the quantification of various kinase activities. Data were shown as mean ± SD (n = 3. All Ns represent independent experiments throughout). (**b**) Phosphorylation of ATM by Cdks *in vitro*. Purified Cdk2, 5, and 6 were incubated with the recombinant GST-ATM4 protein *in vitro* in the presence of [γ-^{32}P]-ATP under manufacturer's recommended conditions (top panel) or with the standard control substrate Histone H1 (bottom panel). (**c**) The effects of dominant negative (dn) Cdks

on CPT-induced γ-H2AX foci formation. CGNs were transfected with constructs for GFP and dnCdks. After 24 hours, cells were treated with 10 μM CPT for 1 hour. γ-H2AX (red) and GFP (green) were detected by immunocytochemistry, and nuclei were labeled with Hoechst (blue). The scale bar represents 5 μM. The average number of foci counted blindly are: GFP control, 0.22; CPT+GFP, 4.81; CPT+dnCdk2, 4.56; CPT+dnCdk5, 3.25, $p<0.001$; and CPT+dnCdk6, 4.44. (**d, e**) Effects of Cdk5 inhibition on the levels of Cdk2 and 6 transcripts. CGNs were treated with 10 μM CPT for the indicated times with or without 10 μM roscovitine. Cdk2 and Cdk6 mRNA levels were quantified by qRT-PCR. Data are shown as mean ± SD (n = 3). (**f**) Inhibition of CPT-induced cell cycle re-entry by roscovitine. CGNs were treated by 10 μM CPT with or without 10 μM roscovitine (Ros) for 8 hours. The percentages of S phase neurons were measured by flow cytometry. (**g**) Inhibition of CPT-induced cell cycle re-entry by knocking down Cdk5. CGNs were infected with Cdk5 RNAi or control lentivirus for 72 hours. The infected cells were treated by 10 μM CPT for 8 hours. The percentages of S phase neurons were measured by flow cytometry. For both **f** and **g**, data are shown as mean ± SD (n = 3. *, $P< 0.05$. **, $P<0.01$).

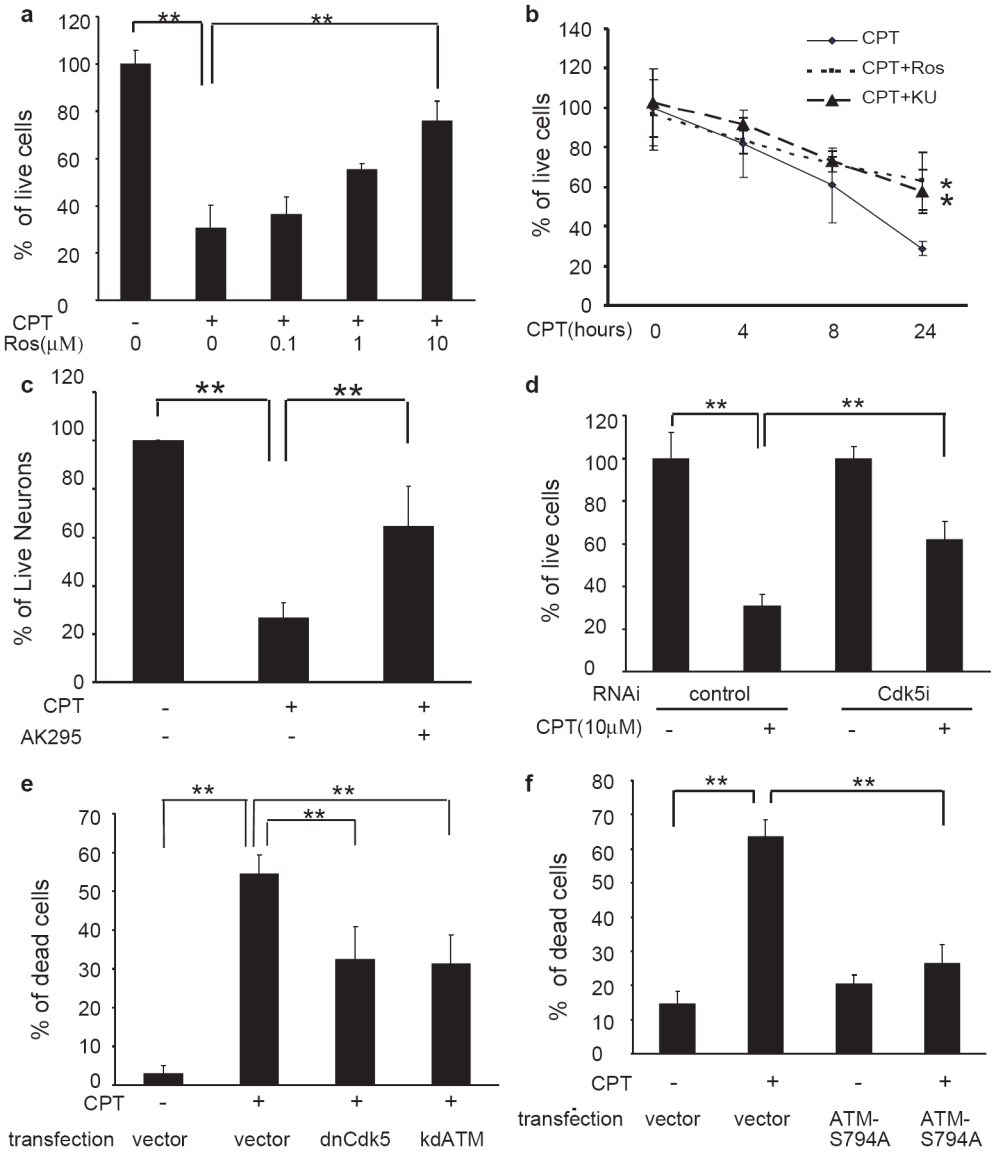

Figure 5. Cdk5-ATM signal regulates DNA damage-induced neuronal death

(**a**) Inhibition of CPT-induced neuronal death by roscovitine. CGNs were exposed to 10 μM CPT and different concentrations of roscovitine for 24 hours. Neuronal viability was measured by WST-1 assay. (**b**) Time dependent effect of roscovitine on CPT-induced neuronal death. CGNs were treated 10 μM CPT alone or with 10μM roscovitine (Ros) or 10 μM Ku-55933 (KU) for the different periods of time. WST-1 data are mean ± SD (n =4. **, $p < 0.01$). (**c**) Inhibition of CPT-induced neuronal death by calpain inhibitor AK295. CGNs were exposed to 10 μM CPT for 24 hours with 50 μM AK295. Neuronal viability was measured by WST-1 assay. (**d**) Effect of knocking down Cdk5 on CPT- induced neuronal death. CGNs were infected with Cdk5 RNAi or control lentivirus for 72 hours and then treated by 10 μM CPT for 24 hours. Neuronal viability was measured by WST-1 assay. WST-1 data are mean ± SD (n =4. *, $p < 0.05$; **, $p < 0.01$). (**e**) Effect of inhibiting Cdk5 or ATM on CPT-induced neuronal death. CGNs were co-transfected with vectors for GFP and

dnCdk5 or kinase-dead ATM (kdATM) as indicated. After 24 hours, cells were treated by 10 μM CPT for 24 hours, and stained by EthD1. Cell death was scored blindly and calculated as described in methods. (**f**) Effect of ATM-S794A on CPT-induced neuronal death. Neurons differentiated from SH-SY5Y cells were co-transfected with vectors for GFP and ATM-S794A as indicated. Following CPT treatment, single cell survival assay was performed as described in (e). For **e** and **f**, data are shown as mean ± SD (n=4. ** $p<0.01$).